

DOI: 10.1002/ ((please add manuscript number))

Full Paper

Contrasting Electrochemical Behaviour of CuO Nanoparticles as Ensembles and as Single Entities: Implications for the Assessment of their Environmental Fate

Giorgia Zampardi , Jorg Thöming, Hendrik Naatz, Hatem M.A. Amin, Suman Pokhrel, Lutz Mädler, and Richard G. Compton**

Dr. G. Zampardi, Dr. H. M. A. Amin, Prof. Dr. R. G. Compton
Department of Chemistry, Physical and Theoretical Chemistry Laboratory, University of Oxford, South Parks Road OX1 3QZ, Oxford, United Kingdom.
E-mail: richard.compton@chem.ox.ac.uk

Prof. Dr. J. Thoeming
Centre for Environmental Research and Sustainable Technology, University of Bremen, 28359 Bremen, Germany
Department of Production Engineering, University of Bremen, Badgasteiner Str. 1, 28359 Bremen, Germany.

H. Naatz, Dr. S. Pokhrel, Prof. Dr. L. Maedler
Department of Production Engineering, University of Bremen, Badgasteiner Str. 1, 28359 Bremen, Germany.
Leibniz Institute for Materials Engineering IWT, Badgasteiner Str. 3, 28359 Bremen, Germany.

E-mail: thoeming@uni-bremen.de , richard.compton@chem.ox.ac.uk

Keywords: single copper oxide nanoparticles electrochemistry, cyclic voltammetry, environmental fate, chloride ions, nitrate ions

The electrochemical behaviour of copper oxide nanoparticles is investigated at both the single particle and at the ensemble level in neutral aqueous solutions through the electrode-particle collision method and cyclic voltammetry, respectively. The influence of Cl^- and NO_3^- anions on the electrochemical processes occurring at the nanoparticles is further evaluated. The electroactivity of CuO nanoparticles is found to differ between the two types of experiments. At the single particle scale, the reduction of the CuO nanoparticles proceeds to a higher extent in presence of chloride ion than of nitrate ion containing solutions. However, at the multi-

particle scale the CuO reduction proceeds to the same extent regardless of the type of anions present in solution. The implications for assessing realistically the environmental fate and therefore the toxicity of metal based nanoparticles in general, and copper based nanoparticles in particular, are discussed.

1. Introduction

Many industrial sectors embrace nowadays the use of a variety of nanoparticles (NPs), ranging from metal, metal oxide to organic based NPs, leading to an increase of their global production and consumption over the last years^{1,2}. The functionalities of the engineered metal based nanoparticles depend strongly on the redox state of their metallic constituents. This is especially relevant for copper based NPs which are used in many chemical and physicochemical processes such as catalysis^{3,4}, electrocatalysis⁵ and sensors⁶⁻⁸. Moreover, copper based nanoparticles are employed in numerous industrial applications ranging from plants protection⁹ to antifouling⁸, as well as in many biological applications as antimicrobial agents¹⁰ and biosensors¹¹. Because of their wide range of applications, copper based nanoparticles are thought to be discharged into the environment through industrial effluents and waters, therefore coming in contact with living organisms¹². In order to understand the fate of the nanoparticles dispersed in the environment and hence to assess the toxicity of metal based NPs in general¹³ and copper based NPs in particular¹⁴⁻¹⁶, it is of crucial importance to study their redox chemistry and the consequent species transformation¹⁷. In fact, it is already known that CuO nanoparticles can cause the generation of intracellular reactive oxygen species (ROS) such as hydrogen peroxide, together with free hydroxyl and superoxide radicals^{18,19}. When produced in excess, ROS species are responsible for enhancing the oxidative stress inside the cells and therefore can lead to their death¹⁸. Whilst it is debated in the literature that the presence of defect sites on the surface of CuO nanocrystals might promote the formation of such reactive oxygen species¹⁹, evidence has been found proving

that the redox activity of the CuO nanoparticles has a critical role in determining the extent of the cell's oxidative stress¹⁸. This is explained on the basis that when a living cell changes its redox conditions, electroactive CuO nanoparticles in contact with it can undergo various degradation reactions leading to a local increase of the concentration of reactive Cu species^{18, 20}. In presence of hydrogen peroxide Cu(II) cations can initiate the formation of superoxide radical anions, and Cu(I) cations can cause the formation of hydroxyl radicals through a Fenton-like reaction^{15, 20}. This enhanced ROS formation leads to a great oxidative damage of the cellular components, such as protein, lipids and nucleic acids, and eventually to cell death^{18, 19}. Additionally, it has been shown that CuO nanoparticles can be toxic not only to cells but also to more complex organisms. CuO nanoparticles can be accumulated in the tissues of estuarine and marine organisms, such as the amphipod *Leptocheirus plumulosus*²¹, mussels like *Mytilus galloprovincialis*²², *Mytilus edeli*²³ and in sea urchin²⁴, causing an inhibition of their enzymatic activity, embryonic development, defence mechanisms, and when present at high concentration, death of the organism.

To date, the nanoparticles redox activity is conventionally evaluated through cyclic voltammetry of films of nanoparticles immobilized onto the electrodes surface^{5, 14, 25, 26, 27}. In this way it is possible to assess the governing electron transfer processes together with the chemical species involved, in terms of element composition and oxidation state²⁸. The nanoparticles immobilisation onto the electrodes surface is often obtained either through lamination²⁹ or drop cast³⁰, which results for both cases in multilayer deposits of particles. Whilst this is the purpose of the lamination process, the opposite is true for the drop cast method whose aim is to distribute a small amount of particles as a single or a few monolayers. However, during the evaporation step in the drop cast procedure particles clogging forming coffee ring like structures³¹ is usually observed. Because of the multilayer deposits onto the electrode surface, any precise quantification of the particle properties through the analysis of the cyclic voltammograms requires detailed knowledge of the intra particles contact resistance

and how this modifies the electron transfer processes, especially for the case of poorly conductive nanoparticles. Moreover, it is worth noticing that the electrochemical analysis of a particle ensemble does not reflect necessarily the behaviour of the material at the single particle level and this can lead to deceptive conclusions on the fate of the nanoparticles dispersed in the environment and, as a consequence, on estimating their toxicity.

In contrast, the electrode-particle collision method, often referred to as “nanoimpacts”, does not necessitate *a priori* information about the nature of the infra-particle contact resistance, and it allows the investigation of the electrochemical behaviour of the nanoparticles as *single entities*. This method consists in dispersing nanoparticles in solution which may, by virtue of their Brownian motion, stochastically collide against a polarised microelectrode surface, producing spikes in the background current recorded at the microelectrode³². The measurement of the Faradaic current deriving from the particles collisions allows a rapid and stochastic detection of a large number of individual particles. The magnitude of the charge, duration and frequency of a numerically relevant number of single impact events, leads to the direct information of the reaction occurring at the nanoscale³². The electrode-particle collision technique has been applied to several fields from electrocatalysis^{33, 34} to energy storage and conversion^{35, 36}, and it was proven to be effective in facilitating the study of the reactivity of *individual* particles.

In this study the electrochemical behaviour of copper oxide nanoparticles was analysed in neutral solutions containing different salts. At first the more commonly used cyclic voltammetry was employed to study the material at the ensemble level. The results were then compared to the behaviour of the material at the single particle level, whose conditions approach more closely the ones of the nanoparticles when they are dispersed in the environment.

2. Results and Discussion

2.1. CuO nanoparticles characterisation

The BET measurement showed that CuO nanoparticles had a $83.6 \text{ m}^2/\text{g}$ specific surface area which corresponds to an average of 11.4 nm primary particle size. The XRD measurement of the fine powder was very crystalline with clear XRD patterns assigned to CuO. Similarly, the TEM overview showed 10 nm crystallite sizes for CuO with spherical morphology (Figure S1).

2.2. CuO nanoparticles ensemble behaviour

The voltammetric behaviour of the copper oxide nanoparticles as an ensemble was studied by modifying the surface of a glassy carbon electrode through drop-casting $4.5 \text{ }\mu\text{g}$ of pure copper oxide nanoparticles from a solution containing 1 g/L of CuO NPs dispersed in water by sonication with a sonic horn as described within the experimental section. In order to estimate the influence of some anionic species most commonly found in water streams on the redox processes occurring at the nanoparticles, the cyclic voltammetries were performed in different electrolytes containing KNO_3 and KCl . From the SEM images of the same amount of CuO nanoparticles drop-casted onto a glassy carbon plate and dried under a nitrogen flow (Figure S2) it was possible to estimate the particle size distribution (Figure S2c) and consequently the average NPs diameter, which was found to be $195 \pm 88 \text{ nm}$ considering the mean, or $182 \pm 88 \text{ nm}$ considering the median of the distribution. Such big particles are most likely formed by the aggregation of many primary crystallites with c.a. 10 nm diameter as observed through TEM analysis (Figure S1a). In fact, the particles that are synthesised

through flame spray pyrolysis are characterised by a highly porous nature, with a void fraction generally around 90%³⁹.

It is worth noticing that considering the average particle diameter and 4.5 µg of CuO NPs drop-casted onto a glassy carbon electrode having a radius of 1.5 mm, less than one monolayer (i.e c.a. 0.75 monolayer) of CuO nanoparticles are deposited onto the electrode surface. Nevertheless, Figure S2a shows a significant clustering which is likely due to the particle aggregation/agglomeration upon drying.

The voltammetric response of the CuO NPs modified glassy carbon electrode is shown in **Figure 1**. Starting from the open circuit potential, the electrode was swept cathodically in order to reduce the copper oxide nanoparticles. Considering the reductive charge recorded in the two solutions, it appears that in presence of chloride ions the CuO nanoparticles present on the electrode surface undergo a one electron reduction, whilst in presence of nitrate ions the reduction of the CuO nanoparticles appears to be a two electron process. The NO_3^- and Cl^- anions, in fact, are expected to influence the redox processes of copper, promoting a direct two electron transfer reduction from Cu(II) to Cu(0) in the case of nitrates solutions, and one electron transfer reduction from Cu(II) to Cu(I)-Cl species, respectively⁴⁰⁻⁴⁴. It is worth noticing that in presence of nitrates there is a pronounced oxidative peak which is ascribed to the stripping of Cu(0) formed during the direct two electron reduction, whilst in presence of chlorides the oxidative peak is much smaller suggesting the formation of soluble Cu(I)-Cl species.

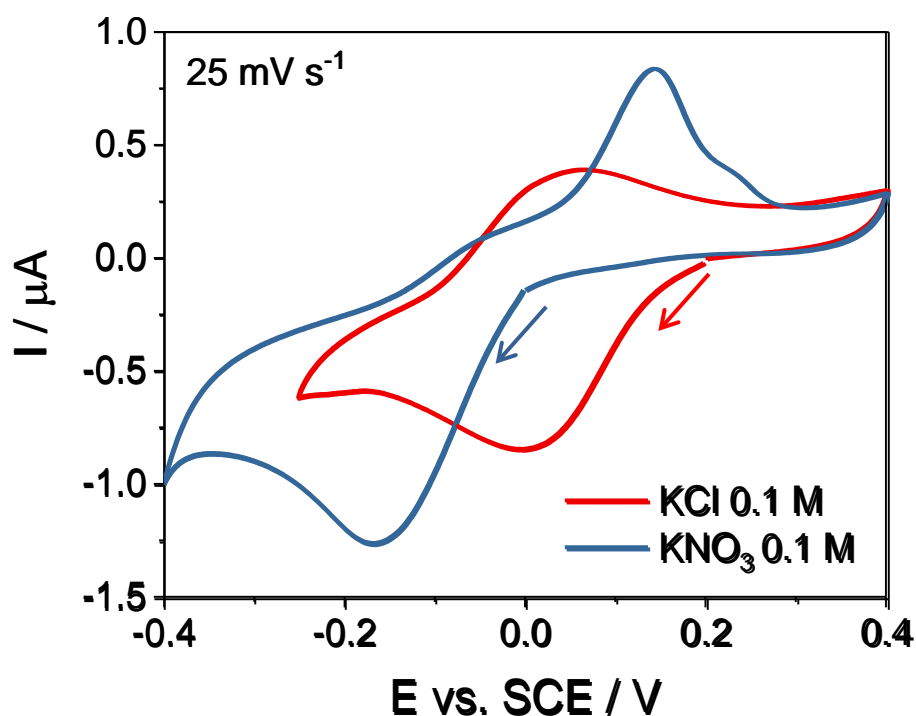


Figure 1: Cyclic voltammograms of a CuO NPs modified glassy carbon electrode in solutions containing KCl 0.1 M (red) and KNO₃ 0.1 M (blue) at a scan rate of 25 mV s⁻¹.

In both cases the measured reductive peak charge, c.a. -6 μC in KNO₃ and c.a. -3 μC in KCl, suggests that only less than 0.1% of the CuO nanoparticles present on the electrode surface are reduced (considering a two electrons and one electron reduction in KNO₃ and KCl containing electrolyte, respectively) leading to the conclusion that CuO nanoparticles have a similar reactivity in both media. The low amount of CuO nanoparticles reacting may be due to a high intra-particle resistance arising from the particle clusters formed upon drying, because of the relatively poor electronic conductivity of copper oxide. For this reason it is likely that only the surface CuO nanoparticles which are in electrical contact with the glassy carbon electrode take part in the reaction.

From the analysis of the cyclic voltammetries recorded at different scan rates (Figures S3, S4, S5, S6), the reduction and oxidation processes occurring at the CuO nanoparticles appeared diffusive in nature in both electrolytic solutions. Considering the small amount of

reacting particles it is likely that the limiting diffusion processes involving point defects or ions take place inside the particle ensemble and not within the liquid phase.

When the cyclic voltammeteries are performed in KCl containing solutions, chloride ions take part to the one electron reduction of the CuO through the formation of Cu-Cl species, as reported previously^{40, 42}. This is further confirmed from the shift in the cathodic peak potential when the cyclic voltammograms are recorded in different KCl concentrations, namely 100 mM, 50 mM, 10 mM, 5 mM and 1 mM KCl (Figure S7a). In order to minimise the ohmic distortion of the voltammograms which would affect the peaks position and shape due to a poor electronic conductivity of the solution, the ionic strength of all the electrolytes was kept constant at 100 mM through the addition of the appropriate amount of KNO₃, which does not affect the reduction of the CuO NPs in the potential range under investigation. In this way it was then possible to estimate the dependency of the peak potential of the Cu(II) to Cu(I) reduction on the logarithm of the chloride concentration (Figure 7b), whose slope was found to be 67 mV/Log [Cl⁻], indicating that the electrode involves the uptake of chloride ions likely producing a copper-chloride complex.

When extending further cathodically the potential range of the cyclic voltammetry (Figure S8), a sharp cathodic peak was observed at around -0.9 V vs. SCE. This peak is much bigger than the one observed at around 0.0 V vs. SCE, which is related to the one electron reduction to form Cu(I)-Cl species (shown in the inset of Figure S8), and it is therefore ascribed to a direct reduction from CuO to metallic copper. The higher cathodic charge of this peak (c.a -5 mC) suggests that around 50 % of the CuO nanoparticles present on the electrode surface take part to such reaction. The oxidative charge is c.a. +4 mC, which means that most of the metallic copper formed upon reduction remains at the electrode. In this case, a greater portion of nanoparticle takes part to the reaction Cu(II) to Cu(0) due to the high cathodic overpotential that is applied to the electrode, which is far more reductive than the thermodynamic potential at which metallic copper is formed^{40, 44}.

2.3. CuO single nanoparticles behaviour

Subsequent to the ensemble measurements, the electrochemical behaviour of single CuO nanoparticles was investigated through the electrode-particle collision method: CuO NPs were suspended in solution and a carbon microelectrode was held at a suitable potential. When 40 pM of CuO nanoparticles were dispersed in solution, clear reductive spikes appeared in the baseline current during the chronoamperograms (**Figure 2**). Such spikes are related to the stochastic arrival of CuO nanoparticles at the microelectrode surface and their subsequent reduction. Within the frame of this work the statistical study of the electrode-particles impacts involved the analysis of more than 4800 spikes, which were recorded in different electrolytic solutions and at different potentials applied to the carbon microelectrode.

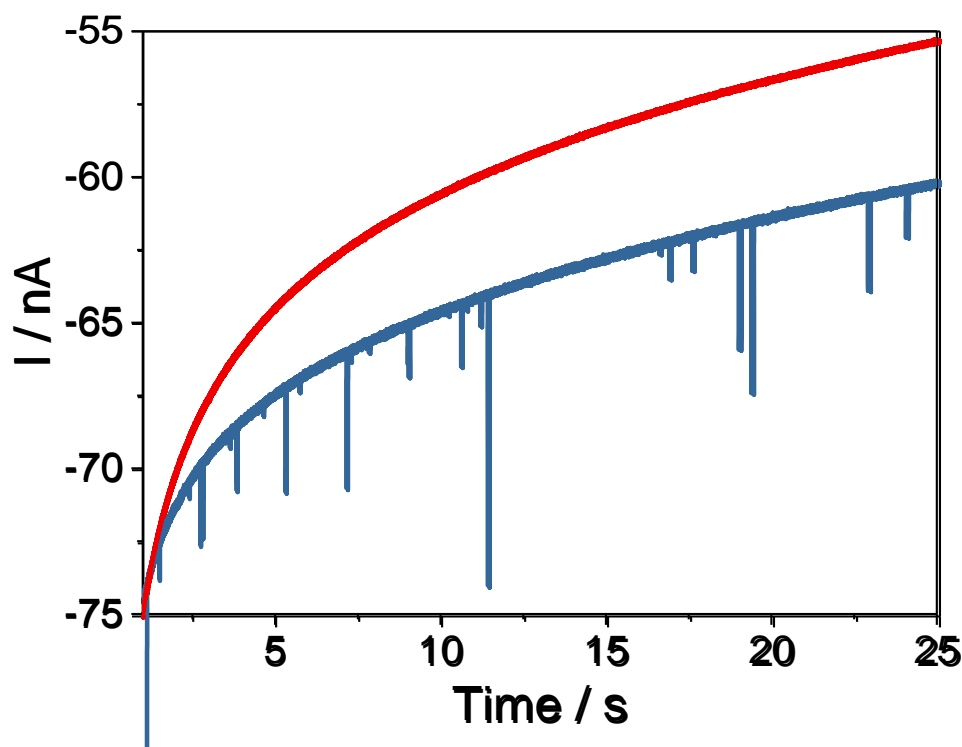


Figure 2: Chronoamperogram of a carbon wire microelectrode in a solution containing 100 mM KCl with (blue line) and without (red line) copper oxide nanoparticle with a concentration of 40 pM. The carbon wire microelectrode was polarised at -0.7 V vs. SCE.

Reductive impacts of CuO nanoparticles were observed starting from a potential of -0.3 V vs. SCE in KNO₃ 100 mM and in different KCl concentrations, namely 5 mM, 100 mM and 1M. During all the collision experiments recorded in a potential range from -0.3 V to -0.7 V vs. SCE a carbon microwire electrode was used³⁸. When the applied potential was -1.2 V vs. SCE a carbon microdisc electrode with a smaller surface area was instead employed, in order to reduce the intensity of the background current and therefore the noise level associated to the measurement.

All the impact experiments were performed within a time frame of no more than 5 minutes after 40 pM of CuO nanoparticles were homogeneously suspended employing an ultrasonic probe (see Experimental section). In order to have an estimation of the stability of the CuO nanoparticles suspended in solutions containing different electrolytes with different concentrations, UV-vis spectra were recorded over an interval of 30 minutes in all the solutions employed during the collision experiments. The suspension underwent severe agglomeration and the nanoparticles precipitated completely after 30 minutes (Figures S9 and S10). The CuO NPs suspension in 5 mM KCl was the most stable in the time frame of the impact experiment, whilst for the one in 1 M KCl the agglomeration rate was much faster probably due to the higher charge screening effect of the electrolyte, which reduces the electrostatic particle-particle repulsion in solution and therefore promotes particle agglomeration.

In all the electrolytic solutions used during the collision experiments, the impact durations were found to be constant and independent of the potential applied to the microelectrode and of the electrolyte concentration (Figures S11 and S12).

In KCl containing solutions the average charge recorded during the impact experiments was found to increase with increasing overpotential, when the carbon microelectrode was polarised more cathodically (**Figure 3**). This effect is not affected by the particles agglomeration, whose rate is unchanged in solutions having the same electrolyte

concentration. The increase of mean impact charge recorded with increasing the KCl concentration (Figure 3a) is most probably the result of two effects: a higher agglomeration rate at higher electrolyte concentration (as shown in Figure S9, S10) and the dependence of the one electron reduction from CuO to Cu-Cl species on the amount of chloride ions in solution.

If the nanoparticles were fully dense, the theoretical charge for completely reduce an average CuO nanoparticle with a diameter of c.a. 195 nm (or 182 nm if the median of the particle size distribution is considered) to Cu(I) species would be c.a. -30 pC (or -24 pC) considering a one electron reduction. Therefore the mean impact charge of -4 pC recorded at -0.7 V vs. SCE in 5 mM KCl would lead to an extent of reduction reaction of the CuO nanoparticles of c.a 10% (or c.a. 15% nm if the median of the particle size distribution is considered). Since it is most likely that the CuO nanoparticles have a void fraction of c.a. 90% (see above), such average impact charge would suggest that the particles undergo a near complete one electron reduction to a Cu-Cl species in 5 mM KCl. Therefore, when further increasing the Cl⁻ concentration in solution, it can be assumed that the CuO nanoparticles undergo a full one electron reduction reaction as well at this strongly negative potential, and the higher average impact charge is a direct consequence of the higher agglomeration rate of the nanoparticles. Therefore it was observed a higher reaction extent at the single particle level compared to the case of the ensemble, where only less than 0.1 % of the particles took part to the reaction.

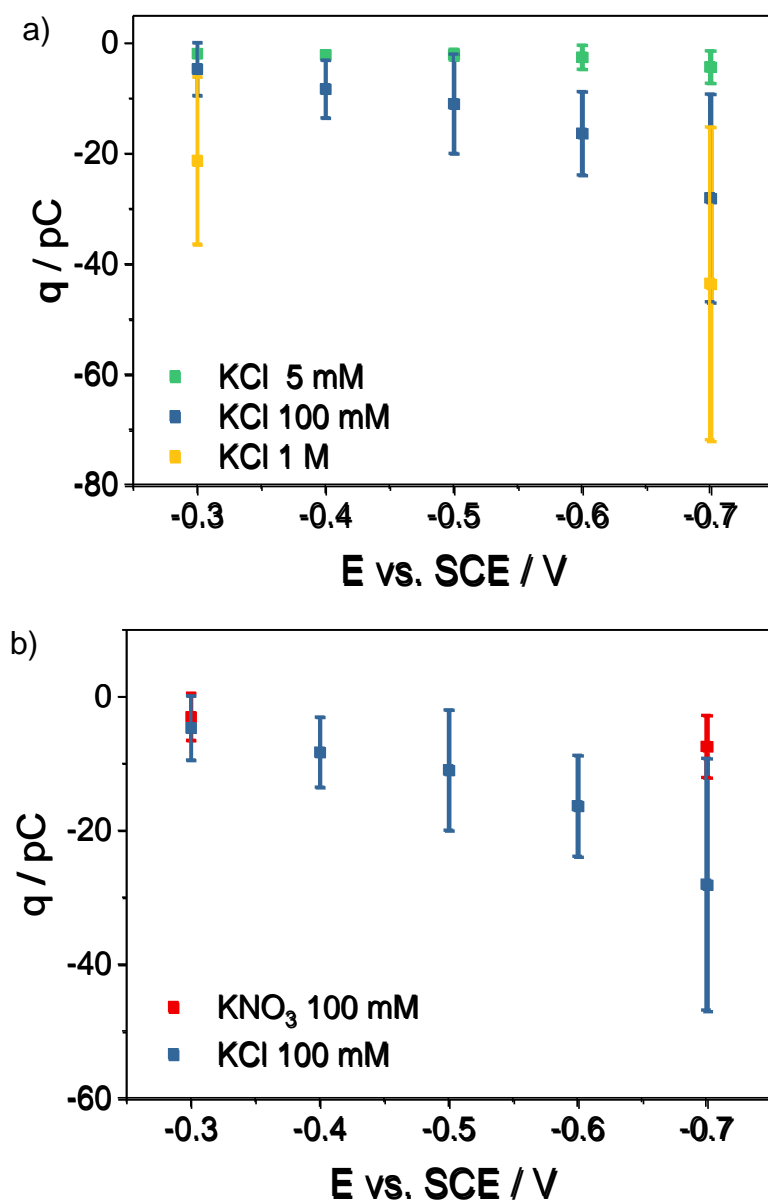


Figure 3: Mean charge of the CuO particles impacts a) recorded in different KCl concentrations; b) comparison between the mean charge recorded in KCl and KNO₃ solutions having the same concentration. CuO particles concentration in solution: 40 pM.

Another difference between the behaviour of the ensemble and the single CuO NPs concerns the extent of reduction involving the nanoparticles in presence of nitrate and chloride ions. From the cyclic voltammetry in Figure 1 it was concluded that the NO₃⁻ and the Cl⁻ anions had an influence on the *nature* of the reaction occurring at the copper oxide nanoparticles, i.e. two and one electron reduction respectively, without however affecting the *extent* of the reactions, i.e. the amount of reacting particles. From the collision experiments

performed in KCl and KNO₃ solutions of the same concentration of 100 mM (Figure 3b) it can be observed that at -0.7 V vs. SCE the average charge for the one electron reduction of CuO in presence of chlorides is much higher than the one measured for the two electron reaction in nitrates.

It is worth noticing that the rate of agglomeration in these two electrolytes can be considered the same in the time frame in which the collision experiments were performed, as demonstrated from the absorbance which decreased of 7 % in KCl and 6.7 % in KNO₃ after 5 minutes (Figure S10c). For this reason, it can be concluded that the extent of reduction of the CuO nanoparticles in presence of nitrate is lower than in presence of chloride ions. Moreover, no dependency of the applied potential on the mean charge recorded during the collision events was observed in nitrate containing solutions. This suggests that at the single particle level the anionic species present in solutions have an effect not only on the nature of the reactions involved, but also on the extent of the reactions occurring at the nanoparticle, and whereas the former effect could be observed through the cyclic voltammetry of the particle ensemble, the latter could not be resolved by the same means.

The distribution of the charge recorded during the collision experiments performed in chloride containing electrolytes was also analysed. Interestingly, the spikes recorded at -0.6 V and -0.7 V vs. SCE in presence of a small concentration of chloride (5 mM KCl) (**Figure 4 a, c**) showed a bimodal distribution that was not observed at any other potentials and KCl concentrations (Figure 4 b, d and Figures S13, S14, S15). To explain such bimodal distribution of the spike charges in Figure 4 a, c, initially it was postulated that the collision events having longer duration likely lead to higher charge, and vice versa. However, the two populations in Figure 4 a were found to have the same average impact duration of c.a. 20 ms. Another explanation of the process leading to the bimodal impact charge distribution might be given considering that a stochastic reaction occurs. When the electrode is polarised at -0.6 V and -0.7 V vs. SCE a portion of the colliding particles may follow the one electron reduction

to form copper-chloride species, whilst for some other particles the reduction may proceed further because of an initiating nucleation of Cu(0).

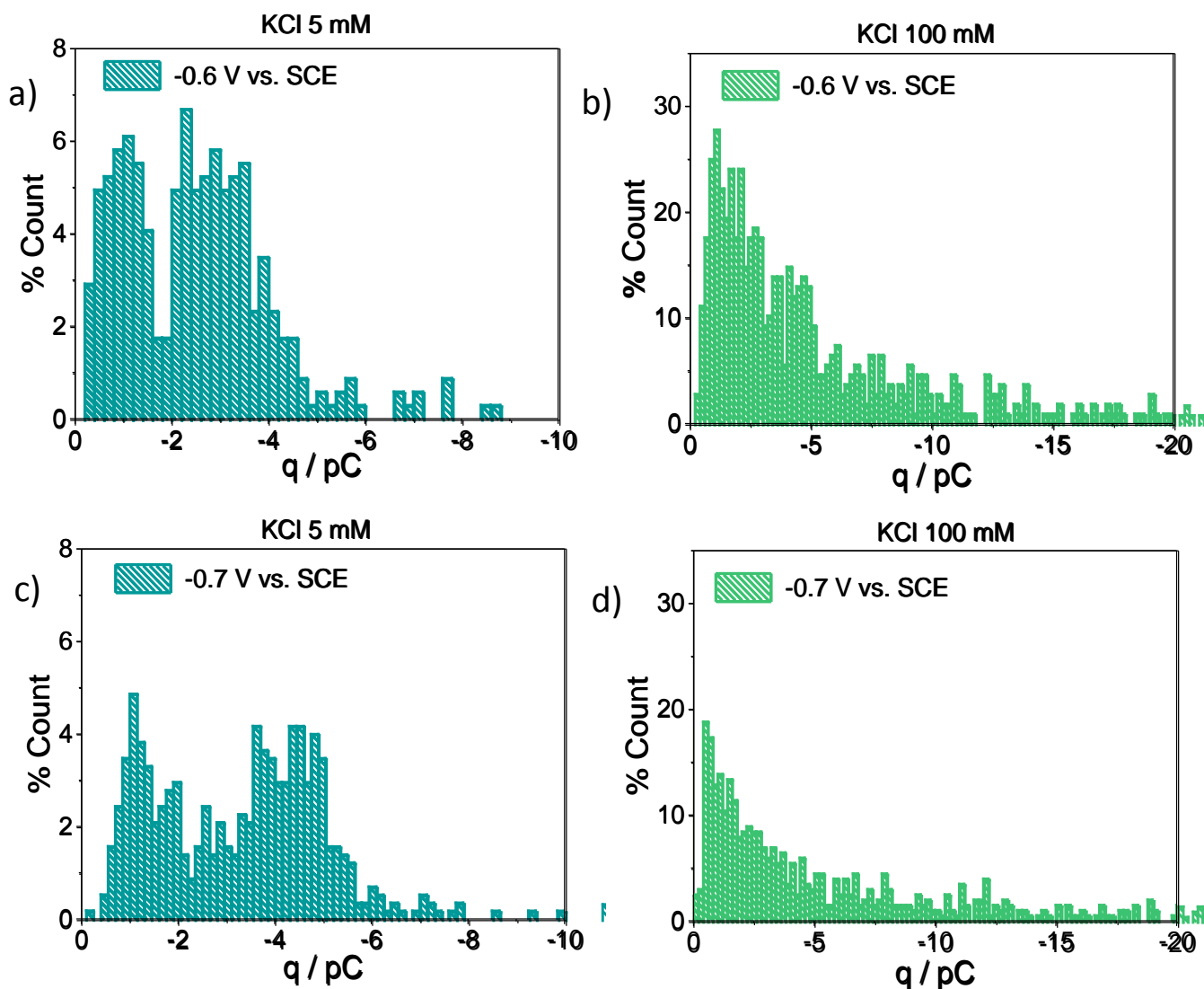


Figure 4: Histograms of the charge recorded during the collision experiments at different potentials in solutions containing 40 pM CuO NPs and a) c) 5 mM or b) d) 100 mM KCl. Counts: a) 344, b) 693, c) 676, d) 830.

The reaction leading to the direct reduction from CuO to metallic copper starts at around -0.55 V vs. SCE (Figure SI16). As any nucleation reaction, such initial Cu(0) formation process has a random nature and it does not take place up to a broad extent unless there are

the conditions which favour the growth process. When the chloride concentration is increased, the impact charge distribution looks monodispersed and such initial nucleation process cannot be resolved anymore. A further evidence of the low extent of this initial copper nucleation reaction can be found in the cyclic voltammeteries recorded at the microelectrode before and after performing the collision experiments recorded in 5 mM and 100 mM KCl at -0.7 V vs. SCE (Figure S17a and S17b): none of the voltammograms show a stripping peak that can be related to a deposit of metallic copper on the electrode surface.

The hypothesis of such Cu(0) nucleation reaction can also explain, together with a more rapid agglomeration, the difference of the mean impact charge recorded at -0.7 V vs. SCE when the collision experiments were performed in 1 M KCl (Figure 3a). In this case the mean impact charge is considerably higher than that measured in lower chloride concentrations. Therefore the nucleation reaction to Cu(0) is inferred to proceed more extensively at such concentrations, when the CuO nanoparticles collide against the polarised microelectrode. This is further confirmed from the cyclic voltammetry recorded at the microelectrode before and after the impact experiments recorded in 1 M KCl at -0.7 V vs. SCE (Figure S17c), which shows a clear stripping peak at around 0 V vs. SCE due to the oxidation of the metallic copper deposited onto the microelectrode during the CuO nanoparticles collisions.

Finally, collision experiments were performed at -1.2 V vs. SCE (**Figure 5a**) in order to assess at the single nanoparticle level the direct two electron reduction from Cu(II) to Cu(0). The mean charge recorded from the impact experiments was -64 pC, double with the respect of the one recorded at -0.7 V vs. SCE of c.a. -30 pC, which suggests that the CuO nanoparticles reacted completely to form metallic Cu(0) (it is worth noticing that being the experiments performed in the same electrolyte concentration, the effect of the particle agglomeration can be excluded in this case). This was further supported by the cyclic voltammetry performed at the carbon microelectrode before and after the collision experiments (Figure 5b). An oxidative peak appears at c.a. 0.3 V vs. SCE indicating that

copper was deposited onto the microelectrode surface upon CuO nanoparticle collisions. Considering all the reductive collisions observed at -1.2 V vs. SCE, a total charge of c.a. -8×10^{-8} C due to the direct two electron reduction from Cu(II) to Cu(0) was recorded. The charge of the oxidative peak observed during the cyclic voltammetry of the microelectrode after the impact measurement (Figure 5b) was c.a. $+7.5 \times 10^{-8}$ C, indicating that almost all the metallic copper formed during the collision experiments remained at the microelectrode surface.

Also in this case, at the single nanoparticle level the direct two electron reduction of CuO nanoparticle was found to proceed to a higher extent than for the case of the particles ensembles, where only c.a. 50% of the particles took part in the same reaction during the cyclic voltammetry.

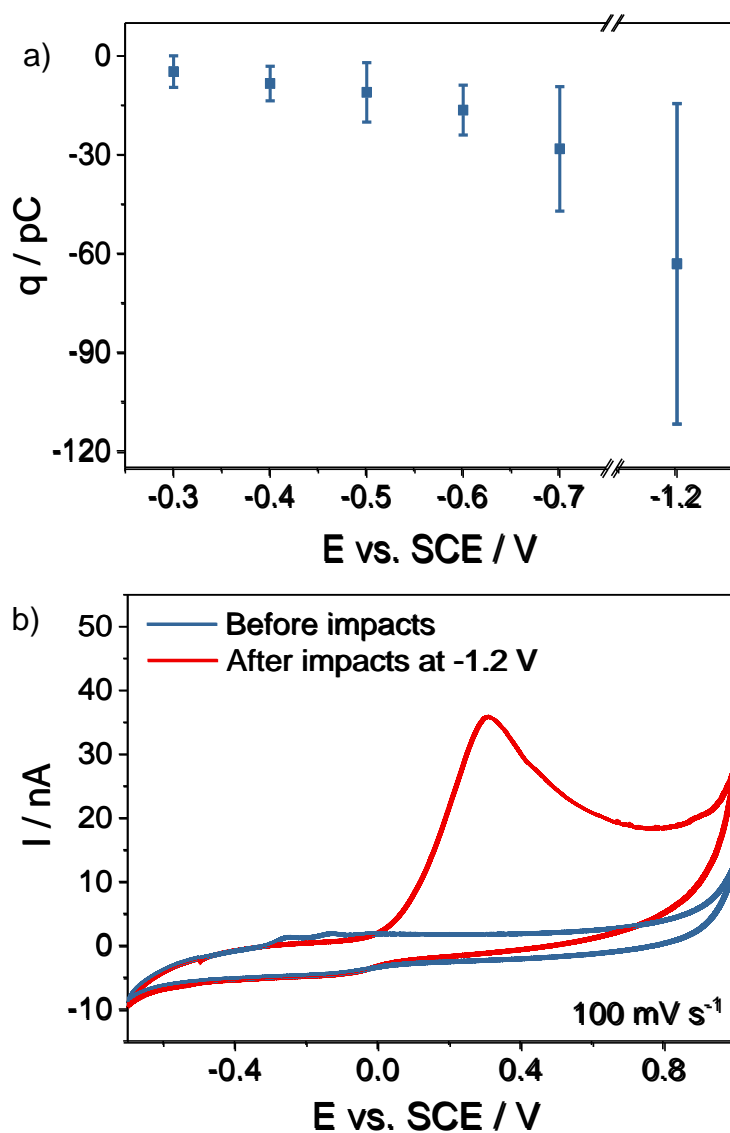


Figure 5: a) mean charge of the CuO nanoparticles impacts recorded in 100 mM KCl at different potentials applied to the carbon microelectrode; b) cyclic voltammetry of the microelectrode in a solution containing 100 mM KCl before (blue line) and after (red line) performing the collision experiments at -1.2 V vs. SCE.

3. Conclusions

Because of their widespread uses, CuO nanoparticles are likely to be discharged in the environment through industrial effluents and waters, and therefore to come into contact with living organisms. As a consequence, it is of critical importance to understand the environmental fate of CuO nanoparticles in order to correctly assess their toxicity, which is related to their redox activity. Here the electroactivity of single CuO nanoparticles was compared to the one at the ensemble level and the influence of anionic species commonly found in water streams (namely Cl^- and NO_3^-) was investigated as well.

The electrochemical behaviour of CuO was found to differ between the ensemble level and the nanoparticle level. As ensembles less than 0.1 % of the particles reacted regardless of the anion present in the electrolytic solution, and the processes appeared diffusion limited. At the nanoscale the CuO reduction occurred up to a much greater extent in presence of chloride rather than nitrate. This striking difference suggests that in order to assess the environmental fate of metal based nanoparticles, experiments involving only a macroscopic ensemble of nanoparticles can lead to deceptive conclusions in terms of the redox activity of the metal based nanoparticles, especially in the case of poorly conductive materials. Whilst voltammograms of layers of such particles can reveal the anion influence on the nature of the reactions involved, single particle investigations are necessary to determine the anion effect on redox conversions of dispersed particles. The electrode-particle collision method is an effective way to assess the electroactivity of single metal based nanoparticles and it was demonstrated to give important and complementary insight to the conventional analysis usually performed on these systems, opening up the possibility of testing the nanoparticles in conditions that are more realistically close to the ones when the nanoparticles are dispersed in the environment.

4. Experimental Section

Materials: Flame spray pyrolysis was used for the production of ultrafine powders of pure CuO nanoparticles. The synthesis was performed using copper naphthenate (Strem Chemicals, 99.9% pure) as metallorganic precursor. The precursor was diluted with xylene (Strem Chemicals, 99.95% pure) to keep the Cu^{2+} concentration at 0.5 M. The solution was then delivered to a nozzle tip through a syringe pump at a flow rate of 5 mL/min followed by atomizing the precursor solution with dispersant O_2 and maintaining a pressure drop of 1.5 bar at the nozzle. The combustion of the dispersed droplets is initiated by the co-delivery of CH_4 and O_2 (1.5 L/min, 3.2 L/min) in order to create a premixed flame.

Potassium Chloride and Potassium Nitrate were obtained from Sigma Aldrich UK and used as received. All solutions were prepared using ultrapure water (Millipore) with a resistivity of 18.2 MWcm at 298 K.

Materials characterisation: For the XRD measurements, the CuO nanoparticles obtained from flame spray pyrolysis were loaded in a PANalytical X'Pert MPD PRO diffracting unit, equipped with Ni-filtered $\text{Cu-K}\alpha$ ($\lambda=0.154$ nm) radiation, $1/4^\circ$ fixed divergence, primary and secondary Soller slit with 0.04 rad aperture, circular sample holder with 16 mm diameter, and X'Celerator detector applying a continuous scan in the range of $20\text{--}80^\circ 2\theta$ and an integration step width of $0.0334^\circ 2\theta$.

For the primary particle size determination, N_2 adsorption-desorption measurements were carried out at 77°K using a Quantachrome NOVA 4000e Autosorb gas sorption system. The NPs were placed in a test cell and were allowed to degas for 2 hours at 200°C in flowing nitrogen. The data were obtained by introducing or removing a known quantity of adsorbing gas in or out of a sample cell containing the solid adsorbent, maintained at a constant liquid nitrogen temperature. The primary particle size was derived using the equation $d_{\text{BET}} =$

$6/(\rho_p \cdot S_A)$, where d_{BET} , ρ_p and S_A are defined as the average diameter of a spherical particle, theoretical density and the measured specific surface area³⁷.

A small amount of the powder was dispersed in 5mL of ethanol (AR grade, Strem) in an ultrasonic bath and sonicated for 5 minutes. A drop of this dispersed colloidal solution was drop casted onto a copper grid coated with carbon film and dried at ambient temperature. The small/ large spots of the sample were scanned for the TEM investigation. High and/or low resolution microscopic imaging of the specimens were carried out using FEI Titan 80/300 microscope equipped with a Cs corrector for the objective lens, a Fischione high angle annular dark field detector (HAADF), GATAN post-column imaging filter and a cold field emission gun operated at 300kV as an acceleration voltage.

Scanning electron microscopy (SEM) imaging was performed by JEOL JSM-6500F Scanning Electron Microscope with an accelerating voltage of 5kV. Sample preparation involved the dropcast of copper oxide particles on a conductive glassy carbon substrate followed by drying under a nitrogen atmosphere. The estimation of the average particle diameter was carried out considering the largest length obtained while trying to draw a circle around each particle. UV-vis absorption spectra were measured through a Shimidazu 1800 UV spectrophotometer.

For the SEM and UV-vis measurements, the CuO NPs were dispersed following the same procedure employed to suspend the nanoparticles prior the nanoimpact experiments.

Nanoimpact experiments: Collision experiments and cyclic voltammetry before and after the nanoimpacts were performed in a three electrode electrochemical cell put inside a double Faraday cage. An in-house built low noise potentiostat was used with a 100 Hz Bessel-type low pass filter. The analog-to-digital and digital-to-analog conversion was provided by a USB-6003 DAQ (National Instruments, Tx, USA). These devices were controlled through a script (Python 2.7) with a graphical user interface and real-time electrochemical data visualization based upon the packages provided in the Enthought Tool Suite (Enthought, TX, USA). When the system was used for the collision experiments, the charge passed during an

impact event is conserved although the current-time response may, at short times, be distorted³². Pt foil and saturated calomel electrodes (SCE) were used as the reference and counter electrodes, and cylindrical microwires electrodes fabricated in-house were used as working electrodes. Briefly, a carbon fibre with a diameter of 7 μm (Goodfellow Cambridge Ltd.) was connected to a conducting metal wire using silver epoxy (RS Components Ltd.) conductive adhesive. The wires were treated at 60 °C in an oven for 30 minutes and then inserted in a plastic pipette tip such that only the carbon fibre was exposed. The plastic tip was sealed together with the carbon fibre/metal wire through a cyanoacrylate adhesive in order to prevent any electrical leakage. All the electrodes were dried overnight at room temperature. The carbon fibre protruding from the sealed plastic tip was finally cut down with a scalpel to a length of approximately 1 mm. Details on such electrodes preparation procedure and their characterisation can be found in ref³⁸. For the collision experiments performed at -1.2 V vs. SCE a carbon microdisc electrode with a 33 μm diameter (ASL, Japan) was used, in order to reduce the background current and consequently the noise during the measurements. In order to homogeneously suspend the copper oxide nanoparticles a VCX400 sonic horn (Sonics and Materials, USA) with a maximal power of 400 W was used with a 3 mm titanium alloy probe. Small volumes (2 mL) of solutions containing the copper oxide nanoparticles were sonicated at 20% of the power amplitude with a pulse mode (3 seconds ON and 3 seconds OFF). All the sonication steps were performed within a NaCl-water ice bath at approximately -10 °C in order to effectively disperse the heat produced through the sonication steps.

Cyclic voltammetry experiments: All cyclic voltammetry was performed in a three electrode electrochemical cell using an Autolab III potentiostat (Methrom Autolab B.V., The Netherlands). For each experiment 4.5 μL of a 1 g/L CuO suspension was drop casted onto a glassy carbon electrode with a diameter of 3 mm (ALS, Japan) and let it dry under a nitrogen flow. The protocol used for the suspension of the CuO nanoparticles was the same as the one

described above in the nanoimpact experiments paragraph. Pt foil (Goodfellow, UK) was employed as a counter electrode and a saturated calomel electrode (SCE, +0.241 V vs. SHE) (ALS, Japan) was used as a reference electrode. Prior to each experiment, all the solutions were vigorously purged with nitrogen in order to reduce the amount of oxygen dissolved.

Supporting Information

Supporting Information is available from the Wiley Online Library or from the author.

Acknowledgements

The research leading to these results has received funding from the European Research Council under the European Union's Seventh Framework Program (FP/2007-2013)/ERC Grant Agreement No. 320403. S.P. and L.M. acknowledge the primary support provided by a U.S. Public Health Service Grant, RO1 ES016746 and infrastructure supported by the National Science Foundation and the Environmental Protection Agency under Cooperative Agreement Numbers DBI 0830117 and 1266377. J.T. thanks the German Research Foundation (DFG) for financial support through the Grant TH 893/21-1. We also thank Prof. A. Rosenauer, University of Bremen, for the TEM imaging.

Received: ((will be filled in by the editorial staff))

Revised: ((will be filled in by the editorial staff))

Published online: ((will be filled in by the editorial staff))

References

1. Gao, Y.; Luo, Z. X.; He, N. P.; Wang, M. K. *Journal of Nanoparticle Research* **2013**, 15, (6).
2. Osterwalder, N.; Capello, C.; Hungerbühler, K.; Stark, W. J. *Journal of Nanoparticle Research* **2006**, 8, (1), 1-9.
3. Rout, L.; Sen, T. K.; Punniyamurthy, T. *Angew. Chem.-Int. Edit.* **2007**, 46, (29), 5583-5586.
4. Martinez-Suarez, L.; Frenzel, J.; Marx, D. *Phys. Chem. Chem. Phys.* **2014**, 16, (47), 26119-26136.
5. Li, C. W.; Ciston, J.; Kanan, M. W. *Nature* **2014**, 508, (7497), 504-+.
6. Wei, Q.; Luo, W. D.; Liao, B.; Liu, Y.; Wang, G. *J. Appl. Phys.* **2000**, 88, (8), 4818-4824.

7. Ahmad, R.; Vaseem, M.; Tripathy, N.; Hahn, Y. B. *Anal. Chem.* **2013**, 85, (21), 10448-10454.
8. Batchelor-McAuley, C.; Wildgoose, G. G.; Compton, R. G.; Shao, L. D.; Green, M. L. H. *Sens. Actuator B-Chem.* **2008**, 132, (1), 356-360.
9. Choudhary, R. C.; Kumaraswamy, R. V.; Kumari, S.; Sharma, S. S.; Pal, A.; Raliya, R.; Biswas, P.; Saharan, V. *Sci Rep* **2017**, 7, 11.
10. Azam, A.; Ahmed, A. S.; Oves, M.; Khan, M. S.; Memic, A. *Int. J. Nanomed.* **2012**, 7, 3527-3535.
11. Chen, W.; Chen, J.; Feng, Y. B.; Hong, L.; Chen, Q. Y.; Wu, L. F.; Lin, X. H.; Xia, X. H. *Analyst* **2012**, 137, (7), 1706-1712.
12. Wigger, H.; Hackmann, S.; Zimmermann, T.; Koser, J.; Thoming, J.; von Gleich, A. *Sci. Total Environ.* **2015**, 535, 160-171.
13. Koser, J.; Engelke, M.; Hoppe, M.; Nogowski, A.; Filser, J.; Thoming, J. *Environ.-Sci. Nano* **2017**, 4, (7), 1470-1483.
14. Naatz, H.; Lin, S. J.; Li, R. B.; Jiang, W.; Ji, Z. X.; Chang, C. H.; Koser, J.; Thoming, J.; Xia, T.; Nel, A. E.; Madler, L.; Pokhrel, S. *ACS Nano* **2017**, 11, (1), 501-515.
15. Aruoja, V.; Pokhrel, S.; Sihtmäe, M.; Mortimer, M.; Mädler, L.; Kahru, A. *Environmental Science: Nano* **2015**, 2, (6), 630-644.
16. Adeleye, A. S.; Pokhrel, S.; Madler, L.; Keller, A. A. *Water Res* **2018**, 132, 12-22.
17. Peng, C.; Xu, C.; Liu, Q. L.; Sun, L. J.; Luo, Y. M.; Shi, J. Y. *Environ. Sci. Technol.* **2017**, 51, (9), 4907-4917.
18. Fahmy, B.; Cormier, S. A. *Toxicol. Vitro* **2009**, 23, (7), 1365-1371.
19. Applerot, G.; Lellouche, J.; Lipovsky, A.; Nitzan, Y.; Lubart, R.; Gedanken, A.; Banin, E. *Small* **2012**, 8, (21), 3326-3337.

20. Sulce, A.; Bulke, F.; Schowalter, M.; Rosenauer, A.; Dringen, R.; Kunz, S. *RSC Adv.* **2016**, 6, (80), 9.
21. Hanna, S. K.; Miller, R. J.; Zhou, D. X.; Keller, A. A.; Lenihan, H. S. *Aquat. Toxicol.* **2013**, 142, 441-446.
22. Gomes, T.; Pinheiro, J. P.; Cancio, I.; Pereira, C. G.; Cardoso, C.; Bebianno, M. J. *Environ. Sci. Technol.* **2011**, 45, (21), 9356-9362.
23. Hu, W. T.; Culloty, S.; Darmody, G.; Lynch, S.; Davenport, J.; Ramirez-Garcia, S.; Dawson, K. A.; Lynch, I.; Blasco, J.; Sheehan, D. *Chemosphere* **2014**, 108, 289-299.
24. Torres-Duarte, C.; Adeleye, A. S.; Pokhrel, S.; Madler, L.; Keller, A. A.; Cherr, G. N. *Nanotoxicology* **2016**, 10, (6), 671-9.
25. Murray, R. W. *Chem. Rev.* **2008**, 108, (7), 2688-2720.
26. Pan, W.; Zhang, X. K.; Ma, H. Y.; Zhang, J. T. *J. Phys. Chem. C* **2008**, 112, (7), 2456-2461.
27. Teo, W. Z.; Ambrosi, A.; Pumera, M. *Electrochemistry Communications* **2013**, 28, 51-53.
28. Laborda, F.; Bolea, E.; Cepria, G.; Gomez, M. T.; Jimenez, M. S.; Perez-Arantegui, J.; Castillo, J. R. *Anal. Chim. Acta* **2016**, 904, 10-32.
29. Schopf, S. O.; Salameh, S.; Madler, L. *Nanoscale* **2013**, 5, (9), 3764-3772.
30. Ivanova, O. S.; Zamborini, F. P. *J. Am. Chem. Soc.* **2010**, 132, (1), 70-+.
31. Shen, X. Y.; Ho, C. M.; Wong, T. S. *J. Phys. Chem. B* **2010**, 114, (16), 5269-5274.
32. Sokolov, S. V.; Eloul, S.; Katelhon, E.; Batchelor-McAuley, C.; Compton, R. G. *Phys. Chem. Chem. Phys.* **2017**, 19, (1), 28-43.
33. Jiao, X.; Lin, C.; Young, N. P.; Batchelor-McAuley, C.; Compton, R. G. *The Journal of Physical Chemistry C* **2016**, 120, (24), 13148-13158.

34. Xiao, X.; Fan, F. R.; Zhou, J.; Bard, A. J. *J Am Chem Soc* **2008**, 130, (49), 16669-77.
35. Zampardi, G.; Batchelor-McAuley, C.; Katelhon, E.; Compton, R. G. *Angewandte Chemie* **2017**, 56, (2), 641-644.
36. Zampardi, G.; Sokolov, S. V.; Batchelor-McAuley, C.; Compton, R. G. *Chemistry* **2017**, 23, (57), 14338-14344.
37. Pokhrel, S.; Birkenstock, J.; Schowalter, M.; Rosenauer, A.; Madler, L. *Cryst. Growth Des.* **2010**, 10, (2), 632-639.
38. Ellison, J.; Batchelor-McAuley, C.; Tschulik, K.; Compton, R. G. *Sensors and Actuators B: Chemical* **2014**, 200, 47-52.
39. Riefler, N.; Mädler, L. *Journal of Nanoparticle Research* **2009**, 12, (3), 853-863.
40. Kear, G.; Barker, B. D.; Walsh, F. C. *Corrosion Science* **2004**, 46, (1), 109-135.
41. Haddou, B.; Rees, N. V.; Compton, R. G. *Phys Chem Chem Phys* **2012**, 14, (39), 13612-7.
42. Awad, S. A.; Kamel, K. M.; Abd El-Hadi, Z.; Bayumi, H. A. *Journal of Electroanalytical Chemistry and Interfacial Electrochemistry* **1986**, 199, (2), 341-350.
43. Degrez, M.; Winand, R. *Electrochimica Acta* **1984**, 29, (3), 365-372.
44. Sandberg, J.; Wallinder, I. O.; Leygraf, C.; Le Bozec, N. *Corrosion Science* **2006**, 48, (12), 4316-4338.

Keyword

C. Author 2, D. E. F. Author 3, A. B. Corresponding Author*

Title

ToC figure ((Please choose one size: 55 mm broad × 50 mm high **or** 110 mm broad × 20 mm high. Please do not use any other dimensions))

Copyright WILEY-VCH Verlag GmbH & Co. KGaA, 69469 Weinheim, Germany, 2016.